Double Layers on Auroral Field Lines

M K Hudson, W. Lotko and E Witt

Space Sciences Laboratory, University of California, Berkeley, CA 94720

ABSTRACT

Time-stationary solutions to the Vlasov-Poisson equation for ion holes and double layers are examined along with particle simulations which pertain to recent observations of small amplitude $e\phi/T_e \sim 1$ electric field structures on auroral field lines Both the time-stationary analysis and the simulations suggest that double layers evolve from holes in ion phase space when their amplitude reaches $e\phi/T_e \sim 1$. Multiple small amplitude double layers which have been seen in long simulation systems and are seen to propagate past the spacecraft may account for the acceleration of plasma sheet electrons to produce the discrete aurora.

We have examined time-stationary solutions to the Vlasov-Poisson equation for ion holes and double layers which pertain to particle simulations we have performed and recent observations in space [*Temerin et al*, 1982] In the simulations, small amplitude $e\phi/T_e \sim 1$ double layers appear to evolve from holes in ion phase space when a current carried by electrons drifting at or near their thermal speed is applied to a long system ~1000 Debye lengths In longer current-driven simulation systems, multiple $e\phi/T_e \sim 1$ double layers evolve [*Sato and Okuda,* 1981]. In contrast, when a potential is applied across a simulation system, whichever $e\phi/T_e$ is applied appears as an isolated double layer which forms at the boundary and propagates into the system [*Hubbard and Joyce,* 1979; *Kindel et al* 1981]

Figure 1 shows an example of small amplitude $e\phi/T_e \sim 1$ double layers and solitary waves observed on the S3-3 satellite at 5000 km over the auroral zone There are two types of

aperiodic structures in the parallel electric field component which appear to be independent of the ion cyclotron wave period in the perpendicular electric field component symmetric solitary wave pulses with no net potential jump and asymmetric pulses which we identify as small amplitude $e\phi/T_e \sim 1$ double layers These structures are observed on the millisecond timescale to propagate past the spacecraft at a velocity greater than 50 km/s For a typical example, the inferred velocity was 80 km/s and the pulsewidth was 4 ms This yields a scale length of 320 m, which is 43 Debye lengths assuming a 10 eV, 10 cm^{-3} thermal electron population. This scale length for the double layer thickness is consistent with the current-driven simulations, as is the spacing of one to a few thousand Debye lengths

The propagation speed, a lower limit of 50-100 km/s, is comparable to both the energetic ion beam speed and the ion acoustic speed in the region where the double layers are observed. These are regions of upward-directed ion beams and downward-accelerated electrons measured by the particle detectors on S3-3. *Temerin et al* [1982] suggest that it is possible to account for a substantial portion of the potential drop necessary to explain the observed particle distributions in the cumulative potential drop of the multiple double layers along an auroral field line. It is not possible to determine the direction of propagation from the double probe measurement, as explained in Figure 3 of *Temerin et al.* [1982]. However, we expect the solitary wave/double layer structures to be tied to the ion beam [*Lotko,* 1981a], which propagates upward relative to the spacecraft Furthermore, the observations allow only the two possibilities illustrated in Figure 2 The downward-pointing smaller amplitude electric field is always seen first, corresponding to a downward-propagating compressional mode or an upward-propagating rarefactive mode. In either case, the net electric field is upward, which is consistent with the particle data *Lotko* [1981] has shown that, in the presence of an upward ion beam, the downward-propagating compressional mode is damped, while the upward-propagating rarefactive mode can be amplified by resonant particles A rarefactive precursor to the double layer is also seen in the current-driven simulations discussed below.

A train of ~150 small amplitude double layers has been seen in one 45 second interval.

One hundred fifty $e\phi / T_e \sim 1$ double layers are adequate to accelerate plasma sheet electrons from 100 eV to 15 keV. Thus, the entire auroral potential drop might be distributed in small amplitude double layers

I. Simulations of Current Driven Double Layers

The preceding S3-3 data looks very much like the small amplitude double layers seen in current-driven simulations in long systems [*Sato and Okuda,* 1980, 1981, *Hudson and Potter,* 1981; *Kindel et al*, 1981]. There have been two distinctly different types of double layer simulations, those in which a potential is applied across the system, and those in which a current is imposed In the former case, whatever potential is imposed appears as a sheath at the boundary, which then detaches and propagates into the system Thus large amplitude $e\phi / T_e >> 1$ double layers are possible when a potential difference is imposed across a bounded system. When a current is imposed, current-driven instabilities result which trap ions Holes in ion phase space with associated negative potential spikes then appear (cf , *Hudson and Potter,* 1981). As noted by *Hasegawa and Sato* [1980], in the presence of a current, such a negative potential spike will reflect some of the electrons carrying the current, resulting in an excess of electrons on one side, a deficit on the other, and a net double layer potential jump. Thus it appears that the ion holes play a crucial role in the formation of double layers in current-driven systems

We have examined the T_e / T_i dependence of double layer formation in a series of current-driven simulations using a system 2048 λ_D long with 32000 particles for an electron drift equal to its thermal speed We find that holes in ion phase space and double layers form for $T_e / T_i = 20$ and 4 but not for $T_e / T_i = 3$ and 1 This result is related to the existence criteria for ion holes discussed below.

II. Analytic Ion Holes and Double Layers

We have examined time-stationary solutions to the Vlasov-Poisson equation for ion holes and double layers using the following distribution functions for free and trapped electrons and

ions

$$f_{if}(v) = AC \exp\left\{-\tfrac{1}{2}[\pm(v^2 + 2\phi)^{1/2} - u_0]^2\right\} \qquad v \gtrless \pm(-2\phi)^{1/2} \tag{1}$$

$$f_{ef}(v) = C \exp\left\{-\tfrac{1}{2}[\pm(v^2 - 2(\phi+\psi)/\theta)^{1/2} + v_0]^2\right\} \qquad v \gtrless \pm[2(\phi+\psi)/\theta]^{1/2}$$

$$f_{it}(v) = AC \exp(-u_0^2/2) \exp\{-(\alpha/2)(v^2 + 2\phi)\} \qquad |v| < (-2\phi)^{1/2}$$

$$f_{et}(v) = C \exp(-v_0^2/2) \exp\{-(\beta/2)\ (v^2 - 2(\psi+\phi)/\theta)\} \qquad |v| < [2(\psi+\phi)/\theta]^{1/2}$$

where $C = 1/\sqrt{2\pi}$ and $A = \exp(-v_0^2/2)\ [F(v_0^2/2, \psi/\theta) + T(\beta, \psi/\theta)]$. A is solved for by evaluating F and T, which are defined in the Appendix. The parameters u_0, v_0, α and β are defined below, $\theta = T_e/T_i$ is the free electron-ion temperature ratio, and the potential varies with increasing x from $\phi = 0$ to $\phi = -\psi$ normalized to the free ion temperature. *Schamel* [1972] first used these distribution functions to study ion acoustic solitons. Subsequently, *Bujarbarua and Schamel* [1981] studied ion holes using Boltzmann electrons, which do not carry the current required to produce double layers in the simulations. Recently, *Schamel and Bujarbarua* [1981] have computed double layer solutions using the above distribution functions with current, but for $\alpha > 0$, which corresponds to an ion beam vs an ion hole in the trapping region This type of solution permits the large amplitude $e\phi/T_e >> 1$ double layers obtained when a potential is applied across the system in simulations and laboratory experiments. We will concentrate on the small amplitude ($e\phi/T_e \sim 1$) double layers which are connected in parameter space to ion hole solutions to the Vlasov-Poisson equation. These are obtained using the full set of distribution functions above for $\alpha < 0$, which corresponds to a depletion of ions in the trapping region. Our primary contribution is to vary the electron drift v_0, as well as T_e/T_i. Other parameters of the solutions are ion drift u_0 and the trapping parameters $\alpha = T_i/T_{it}$ and $\beta = T_e/T_{et}$. While α and β are formally the ratios of free to trapped particle temperatures, they are physically proportional to the density of ions and electrons in the trapping region. Thus, $\alpha(\beta) = 1$ and u_0 (v_0) $= 0$ reduces the trapped distributions in (1) to

Boltzmann, while $\alpha(\beta) > 1$ corresponds to an excess and $\alpha(\beta) < 0$ corresponds to a deficit of particles in the trapping region (cf , Figure 1, *Schamel,* 1972).

Integrating Poisson's equation once yields a simple harmonic oscillator equation for $\phi\ (x)$ in a classical potential $V\ (\phi)$ which determines the spatial dependence of ϕ

$$\tfrac{1}{2}\ (\phi'(x))^2 + V(\phi) = 0 \qquad (2)$$

The Sagdeev potential V for ion holes and double layers is shown in Figure 3. The latter must satisfy $V'(-\phi_{min}) = 0$ while the former need not This is because $V'(\phi)$ is proportional to charge density, since (2) is an integral of Poisson's equation, and there is a net charge density at $-\phi_{min}$ for a soliton On the other hand, the electric field and therefore charge density must vanish at $-\phi_{min}$ for a laminar double layer This imposes the additional constraint $V'\ (-\phi_{min}) = 0$ on double layers, which therefore occupy a subset of ion hole parameter space

In our first study we reproduced *Buyarbarua and Schamel's* [1981] result for Boltzmann electrons Figure 4 is an existence diagram for ion holes in parameter space which agrees with their Figure 7. We present this result because our integration scheme described in the Appendix differs slightly from theirs. The dashed line indicates a cutoff where ion holes become double layer solutions satisfying $V'(-\phi_{min}) = 0$. This and the previous figure suggest that an ion hole growing in amplitude by resonant particle interaction may evolve into a double layer. Increasing $-\phi_{min}$ in Figure 3a can convert the ion hole Sagdeev potential into a double layer Sagdeev potential like Figure 3b However, we emphasize that the calculation of Figure 4 is time-stationary, and the foregoing is merely a plausibility argument to suggest that when the ion hole amplitude becomes sufficiently large, it becomes a double layer.

We have explored the dependence of ion hole and double layer solutions on the parameters $T_e/\ T_i$, $\beta = T_e/T_{et}$ and v_0 For $\beta = 1$ and $v_0 = 0$ corresponding to Boltzmann electrons, increasing $T_e/\ T_i$ to 20 in Figure 5a and decreasing $T_e/\ T_i$ to 4 in Figure 5b does not change the available parameter space for ion hole solutions if one normalizes to $e\phi/\ T_e$ That is, the solutions are always restricted to $e\phi/\ T_e < 1$ for Boltzmann electrons. However, decreasing $T_e/\ T_i$ to 3 in Figure 6 changes the topology to multivalued solutions

We also varied the electron trapping parameter β. In Figure 7 for $\beta = 3$, the parameter space shrinks and $e\phi/T_e \sim 0.4$ is the maximum allowed amplitude for an ion hole or a double layer. In Figure 8 for $\beta = 0.1$, the parameter space expands to allow $e\phi/T_e = 2.5$. For the Boltzmann electron case ($\beta = 1$), the amplitude was always restricted to $e\phi/T_e < 1$. Increasing β increases the density of electrons reflected from the flanks of the ion hole, which may short out the potential and reduce the maximum allowed $e\phi/T_e$, and conversely

Next we examined the v_0 dependence. For $\beta = 1$ and $T_e/T_i = 20$ and 4, Figure 9a and Figure 9b show that the maximum allowed $e\phi/T_e$ is larger for $v_0 = 0.6$ than for $v_0 = 0$ (see Figure 5a, b). The maximum allowed ion hole amplitude $e\phi/T_e$ increases with v_0, but still remains close to unity, even for the large values of $v_0 = 0.6$ and 1 used in the current-driven simulations [*Sato and Okuda,* 1980, *Hudson and Potter,* 1981]. As v_0 approaches unity ($v_0 > 0.8$), double layer solutions are no longer obtained at the maximum amplitude ion hole solution. This result is discussed in the context of current-driven simulations in the following section. For $\beta = 1$ and $T_e/T_i = 3$, the same kind of multivalued solutions are obtained for arbitrary v_0 as in Figure 6.

Finally, we allowed both α and β to assume negative values. No upper limit on ion hole amplitude and no double layer solutions were obtained for this case.

III. Discussion

To study the temporal evolution of an ion hole into a double layer requires examination of the time dependent Vlasov-Poisson equation, obtaining an evolution equation for the particle distribution functions and potential a' la the KdV equation. *Lotko* [1981a] has worked on the nonlinear growth and damping of ion acoustic solitons due to resonant particle interaction, and has shown that compressional ion acoustic solitons can be amplified by interacting with an ion stream, while rarefactive ion acoustic solitons amplify by interacting with an electron stream, which exists in the ion beam frame. *Lotko* [1981b] has shown that the downward-propagating compressive mode in Figure 2a will be damped because it is propagating against the ion beam,

while the upward propagating rarefactive mode in Figure 2b can be amplified. Whether a mode is amplified or damped depends on whether there are more or fewer resonant particles traveling faster than the wave, as in the case of linear Landau growth or damping In the saturated state where there is no further wave particle momentum exchange, it is possible to construct a potential profile which looks like Figure 2b by matching a soliton and double layer solution to the Vlasov-Poisson equation at the potential minimum The foregoing analysis is for ion acoustic solitons. Analysis of the temporal evolution of ion holes is in progress.

The time-stationary analysis in the preceding section is consistent with the simulations we have performed. For example, the ion holes are observed to evolve into double layers with $e\phi / T_e \sim 1$ for $T_e / T_i = 20$ and 4, but neither ion holes nor double layer formation are observed for $T_e / T_i = 3$ and 1, for $v_0 = 1$ initially. Although $v_0 = 1$ initially in our simulations, it drops to $v_0 = 0\,8$ by $\tau = 500\ \omega_{pe}^{-1}$ for $T_e / T_i = 20$, well after ion holes have formed, but before the double layer has formed [*Hudson and Potter,* 1981]

In summary, current-driven simulations done before solitary waves and double layers were seen in the S3-3 data look remarkably like the observations The simulations and time-stationary solutions to the Vlasov-Poisson equation suggest that these small amplitude double layers evolve from holes in ion phase space when the amplitude reaches $e\phi / T_e \sim 1$

References

Bujarbarua, S and H Schamel, Theory of finite-amplitude electron and ion holes, *Journal of Plasma Physics* 25, 515, 1981

Hasegawa, A and T Sato, Theory of formation of double layer, *Bulletin American Physical Society* 25, 844, 1980 and *Phys Fluids,* to be published

Hudson, M K and D W Potter, Electrostatic shocks in the auroral magnetosphere, in *Physics of Auroral Arc Formation* (edited by S I Akasofu and J R Kan), Amer Geophys Union, Wash , D C , p 260, 1981

Hubbard, R F and G Joyce, Simulation of auroral double layers, *J Geophys Res* 84, 4297, 1979

Kindel, J M, C Barnes, and D W Forslund, Anomalous DC resistivity and double layers in the auroral ionosphere, in *Physics of Auroral Arc Formation* (edited by S I Akasofu and J R Kan), American Geophysical Union, Washington, D C, p 296, 1981

Lotko, W, Ion-acoustic soliton propagation and dynamics in auroral plasma, Ph D dissertation, UCLA, 1981a

Lotko, W, Structure of small amplitude double layers in auroral plasma, ES *Trans Am Geophys Union* **62**, 1012, 1981b

Sato, T, and H Okuda, Ion acoustic double layers, *Phys Rev Lett* **44**, 740, 1980

Sato, T and H Okuda, Numerical simulations on ion acoustic double layers, *J Geophys Res* **86**, 3357, 1981

Schamel, H, Stationary solitary, snoidal and sinusoidal ion acoustic waves, *Plasma Physics* **14**, 905, 1972

Schamel, H and S Bujarbarua, Analytical double layers, preprint, 1981

Temerin, M, K Cerny, W Lotko and F S Mozer, Observations of double layers and solitary waves in the auroral plasma, submitted to *Phys Rev Lett*, 1982

IV. Appendix

Our treatment differs from that of *Schamel and Bujarbarua* [1981] in how the velocity distributions are integrated to obtain densities, and in how those densities are integrated to obtain a pseudo-potential In both treatments the relevant functions are integrals over velocity space of the particle distribution functions multiplied by a factor $\exp(w_0^2/2)$, where w_0 is the drift velocity of the particles Our integration of the trapped distribution is the same as that of *Schamel* [1972] and gives a function T related to the plasma dispersion function and the Dawson integral

$$T(x,y) = 2C\exp(xy)\int_0^{\sqrt{2y}} \exp(-xt^2/2)\,dt$$

where $C = 1/\sqrt{2\pi}$ Our treatment differs in the integration of the free population *Schamel* integrates $\exp(v_0^2/2)$ times the free population

$$f_f(v) = C\exp(-\tfrac{1}{2}[\pm(v^2 - 2\phi)^{1/2} + v_0)^2] \quad |v| > (-2\phi)^{1/2} \tag{A1}$$

over velocity space to obtain

$$F(v_0^2/2,\phi) = \exp(v_0^2/2)\,(1 - erf\sqrt{\phi})\exp(\phi) + K(v_0^2/2,\phi) \tag{A2}$$

[*Schamel*, 1972] where

$$K(x,y) = 2/\sqrt{\pi} \int_0^{\pi/2} d\phi \sqrt{x} \cos\phi \exp(-y\tan^2\phi + x\cos^2\phi) \operatorname{erf}(\sqrt{x}\cos\phi)$$

We, however, make a change of variables in the velocity integral $u = \pm(v^2 - 2\phi)^{1/2}$ and use

$$F(v_0^2/2, \phi) = 2C \int_0^\infty du \frac{u}{[u^2 + 2\phi]^{1/2}} \exp(-u^2/2) \cosh(u v_0) \tag{A3}$$

This can be written in two ways

$$F(v_0^2/2, \phi) = \int_0^\infty du \frac{u}{[u^2 + 2\phi]^{1/2}} [\exp(-u^2/2 + u v_0) + \exp(-u^2/2 - u v_0)] \tag{A4a}$$

or

$$F(v_0^2/2, \phi) = -2\sqrt{\phi/\pi} + C\exp(v_0^2/2)\{\int_0^\infty dw([(w + v_0)^2 + 2\phi]^{1/2} + [(w - v_0)^2 + 2\phi]^{1/2})$$
$$\times w\exp(-w^2/2)\} - 2\int_0^{v_0} dw[(w - v_0)^2 + 2\phi]^{1/2} w\exp(-w^2/2) \tag{A4b}$$

In our evaluation, we make the change of variables $u = \sqrt{2}\tan\theta$ to change the infinite limits to a finite interval of zero to 2π, and we numerically integrate this result. (A4a) is used for $v_0 < 4.5$, and (A4b) is used for $v_0 > 4.5$

The difference in evaluation of F also leads to different forms for the integral of F used in the pseudo-potential. *Schamel* integrates (A2) over ϕ for the pseudo-potential, whereas we integrate (A3) over ϕ to find

$$G(v_0^2/2, \phi) = 2C \int_0^\infty du\, u\, [u^2 + 2\phi]^{1/2} \exp(-u^2/2) \cosh(u v_0) \tag{A5}$$

The Sagdeev potential is then

$$V = -\theta\{\theta\exp(-v_0^2/2)[G(v_0^2/2, (\psi + \phi)/\theta) - G(v_0^2/2, \psi/\theta) + D(\beta, (\psi + \phi)/\theta)$$
$$- D(\beta, \psi/\theta)] + A\exp(-u_0^2/2)[G(-u_0^2/2, -\phi) - G(-u_0^2/2, 0) + D(\alpha, -\phi)]\}$$

where $D(x,y) = (T(x,y) - 2\sqrt{y/\pi})/x$.

For $v_0 \leqslant 4.5$, (A5) is integrated just as is F in (A4a) For $v_0 > 4.5$, we use a method similar to that used in (A4b)

The small amplitude expression for our F agrees with that of *Schamel* [1972] and the numerical evaluation of F agrees with the small amplitude expansion to better than 1 part in 10^5 The numerical evaluation of G agrees with the small amplitude expansion to better than 1

part in 10^8.

Figure Captions

Figure 1 The two perpendicular and one parallel electric field components shown Examples of double layers (DL), solitary waves (SW) and electrostatic ion cyclotron (EIC) waves are marked

Figure 2 (a) Downward propagating compressive and (b) upward propagating rarefactive modes consistent with S3-3 electric field data I is ionosphere and M is magnetosphere

Figure 3 Sagdeev potential V defined by (2) for (a) ion holes and (b) double layers

Figure 4 Existence diagram for ion holes assuming Boltzmann electrons α is the ratio of free to trapped ion temperature and u_0 is the free ion drift in the wave frame normalized to its thermal speed Negative α corresponds to a deficit of trapped ions (hole), see (1) The dashed line corresponds to double layer solutions

Figure 5 (a) Same as Figure 4 for $T_e/T_i = 20$ (b) Same as Figure 4 for $T_e/T_i = 4$

Figure 6 Same as Figure 4 for $T_e/T_i = 3$, except that solutions are now multi-valued where curves cross, while end points satisfy double layer criterion $V'(-\phi_{min}) = 0$

Figure 7 Same as preceding figures with $\beta > 1$, which corresponds to an excess of electrons over the Boltzmann level in the trapping region β is the ratio of free to trapped electron temperature, proportional to the density of trapped electrons (see (1))

Figure 8 Same as Figure 7 with $\beta < 1$, which corresponds to a deficit of electrons relative to the Boltzman level in the trapping region

Figure 9 (a) Same as Figure 5a with $v_0 = 0.6$, where v_0 is the free electron drift in the wave frame normalized to its thermal speed (b) Same as Figure 5b with $v_0 = 0.6$

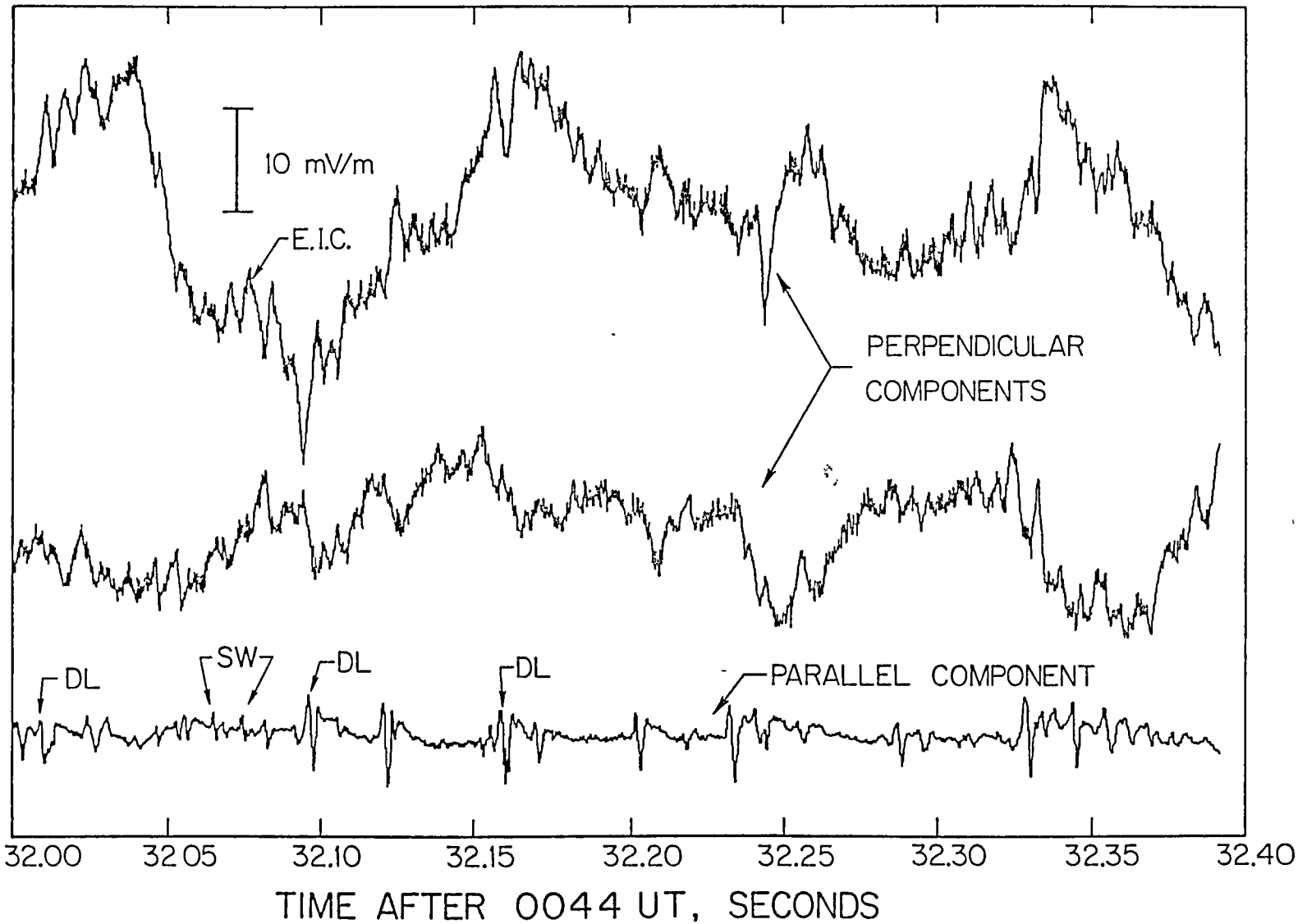
10 mV/m
E.I.C.
PERPENDICULAR
COMPONENTS
DL
SW
DL
DL
PARALLEL COMPONENT
32.00
32.05
32.10
32.15
32.20
32.25
32.30
32.35
32.40
TIME AFTER 0044 UT, SECONDS

Fig. 1

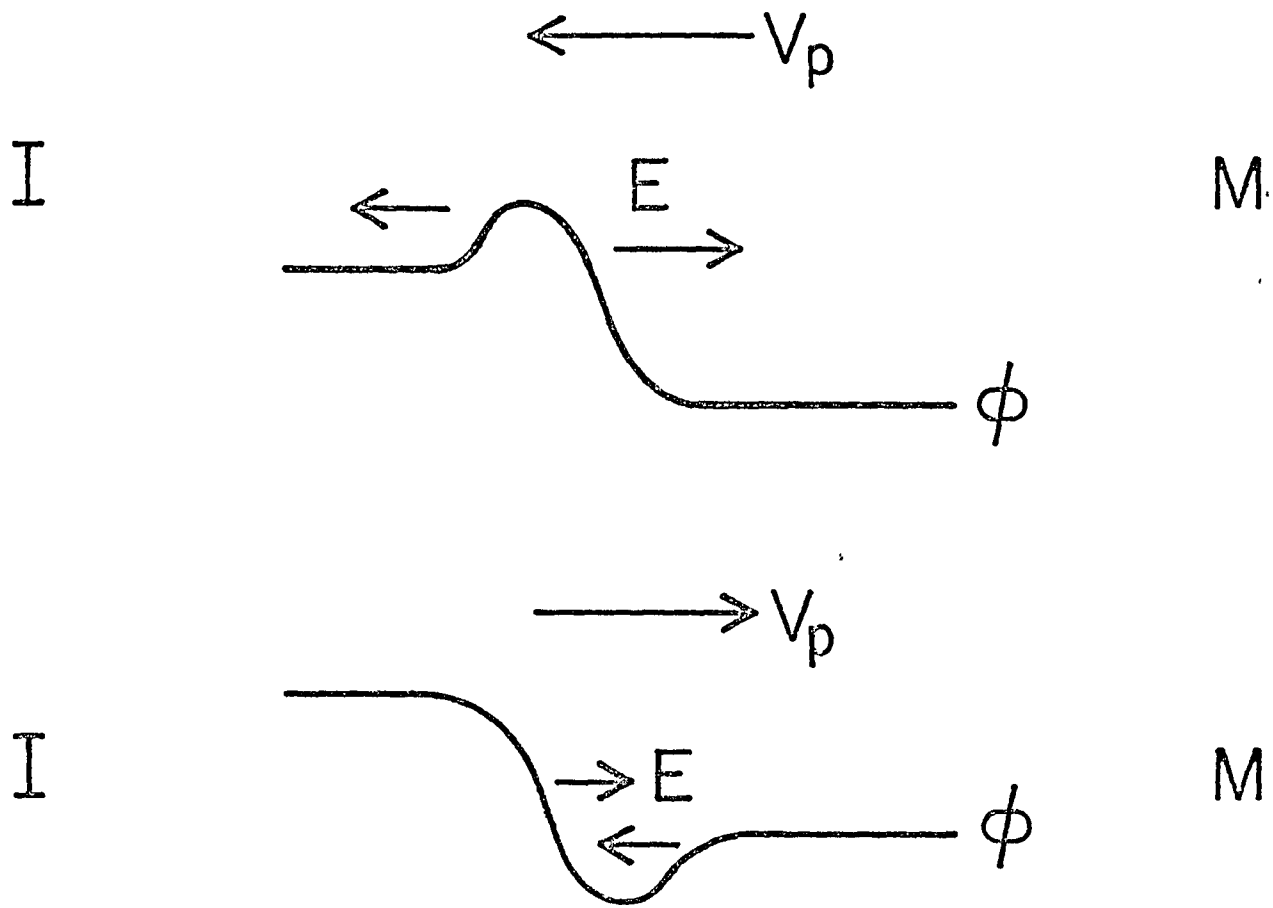

Fig. 2

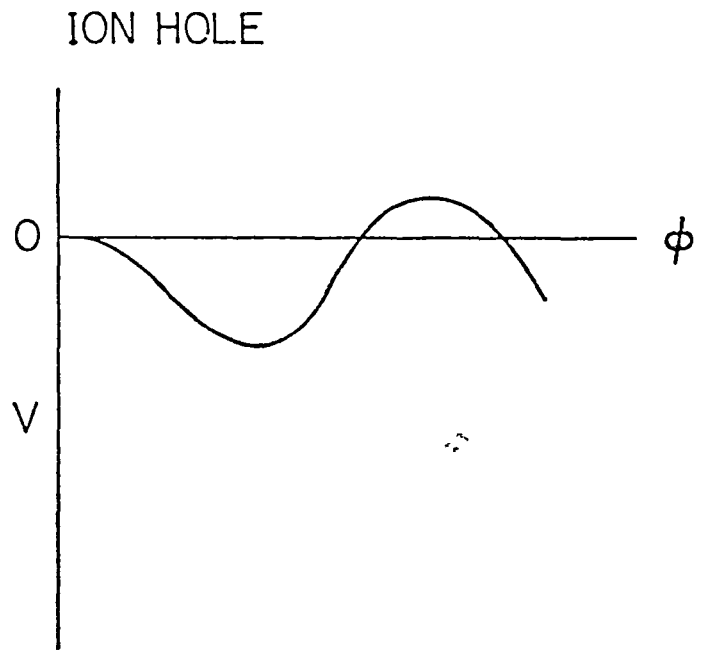

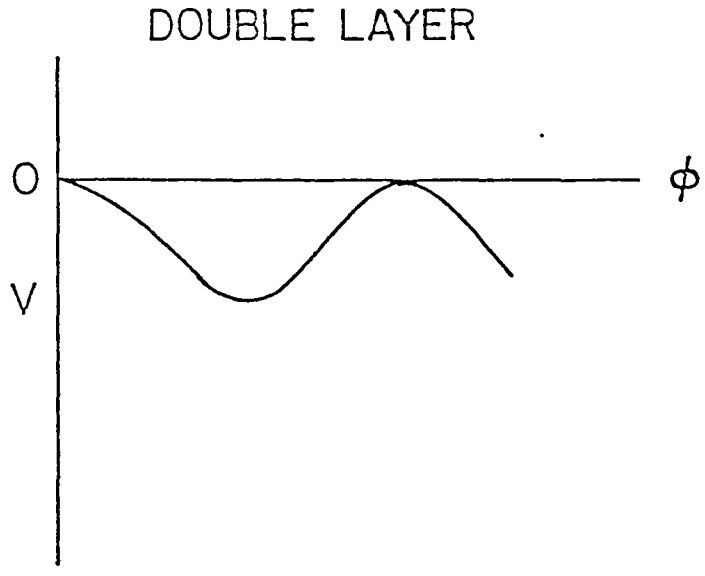

Fig. 3

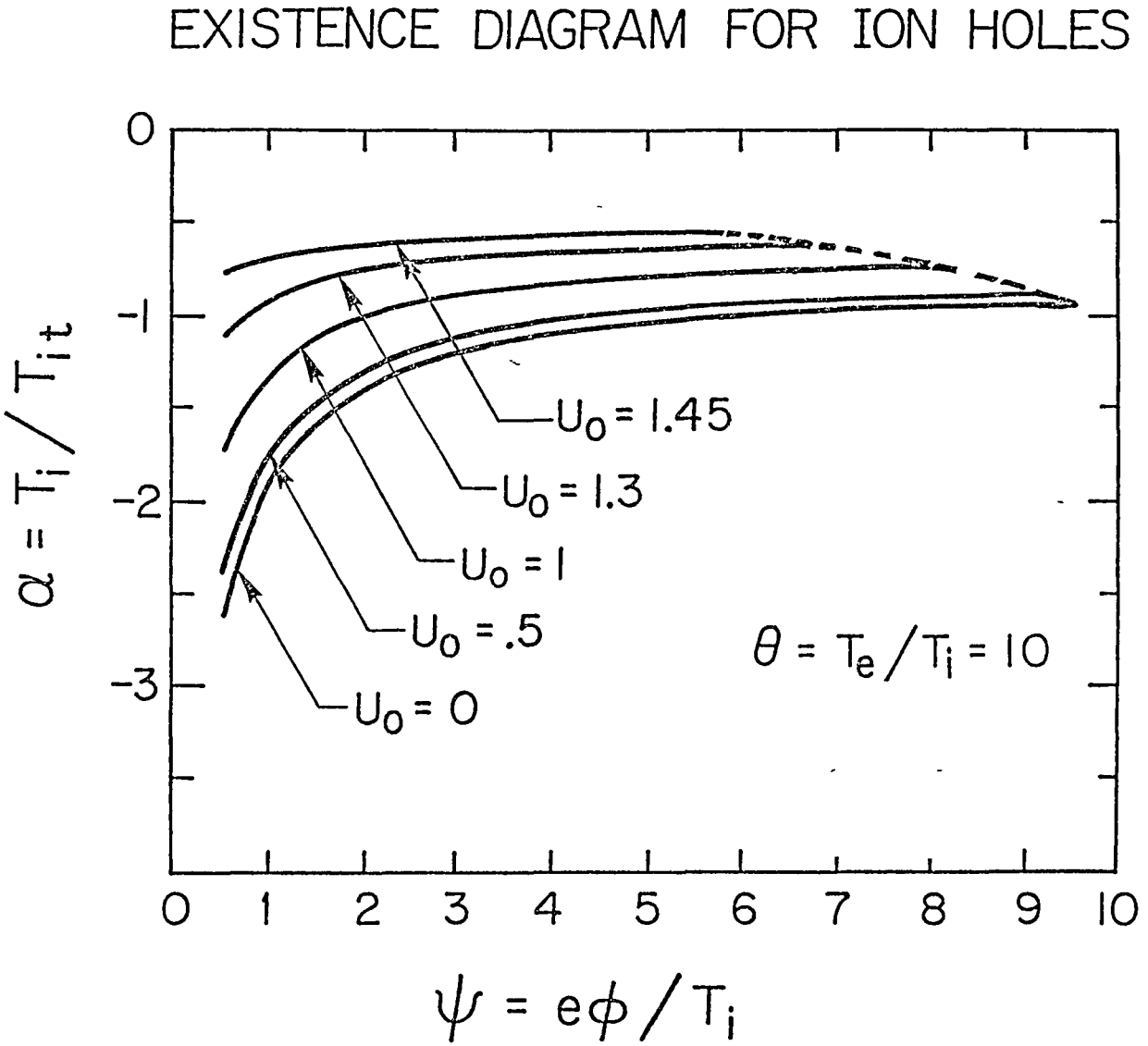
EXISTENCE DIAGRAM FOR ION HOLES
0
-1
-2
-3
$\alpha = T_i / T_{it}$
$U_0 = 1.45$
$U_0 = 1.3$
$U_0 = 1$
$U_0 = .5$
$U_0 = 0$
$\theta = T_e / T_i = 10$
0 1 2 3 4 5 6 7 8 9 10
$\psi = e\phi / T_i$

Fig. 4

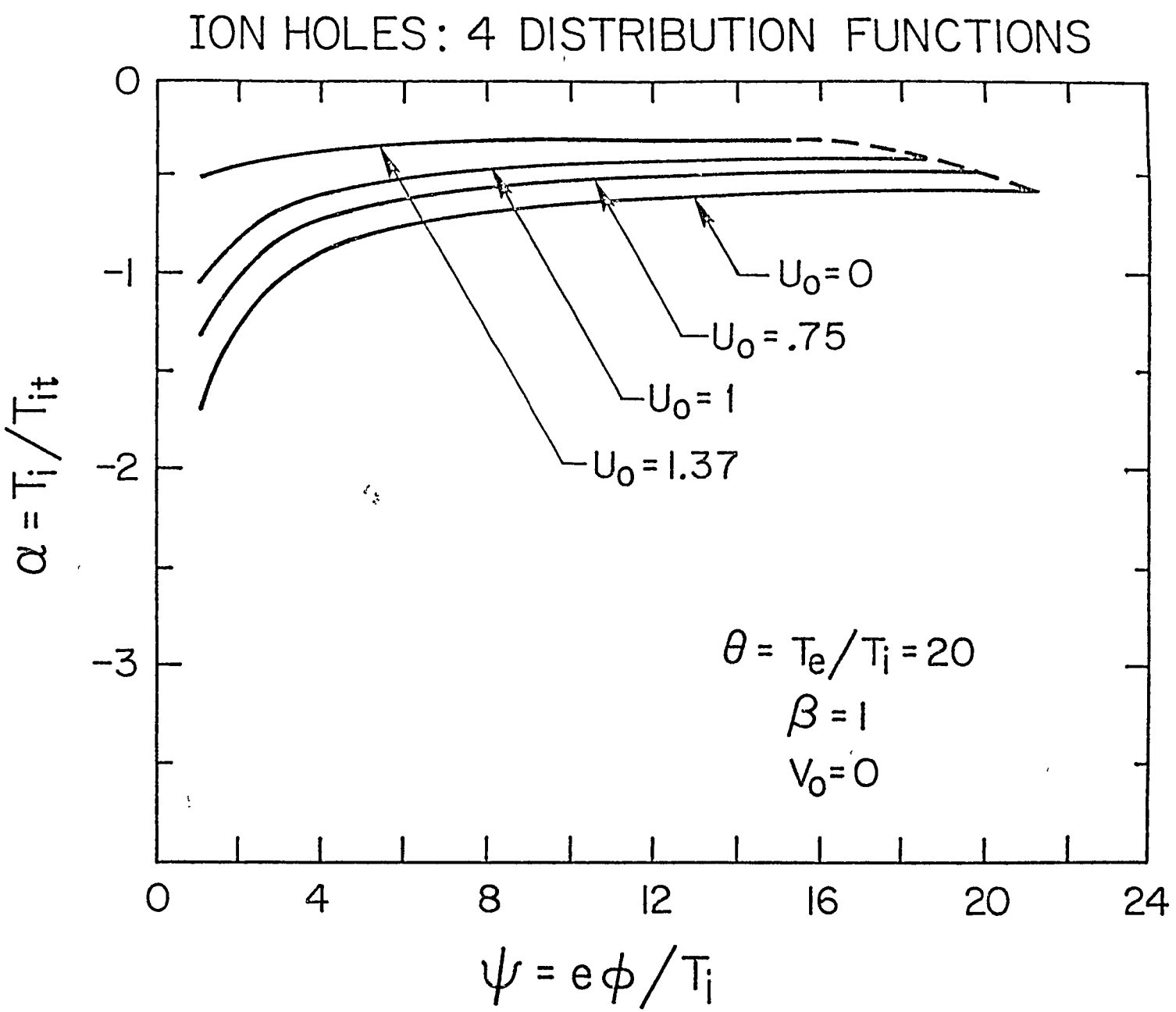
ION HOLES: 4 DISTRIBUTION FUNCTIONS
0
-1
-2
-3
$\alpha = T_i/T_{it}$
$U_0 = 0$
$U_0 = .75$
$U_0 = 1$
$U_0 = 1.37$
$\theta = T_e/T_i = 20$
$\beta = 1$
$V_0 = 0$
0
4
8
12
16
20
24
$\psi = e\phi/T_i$

Fig. 5a

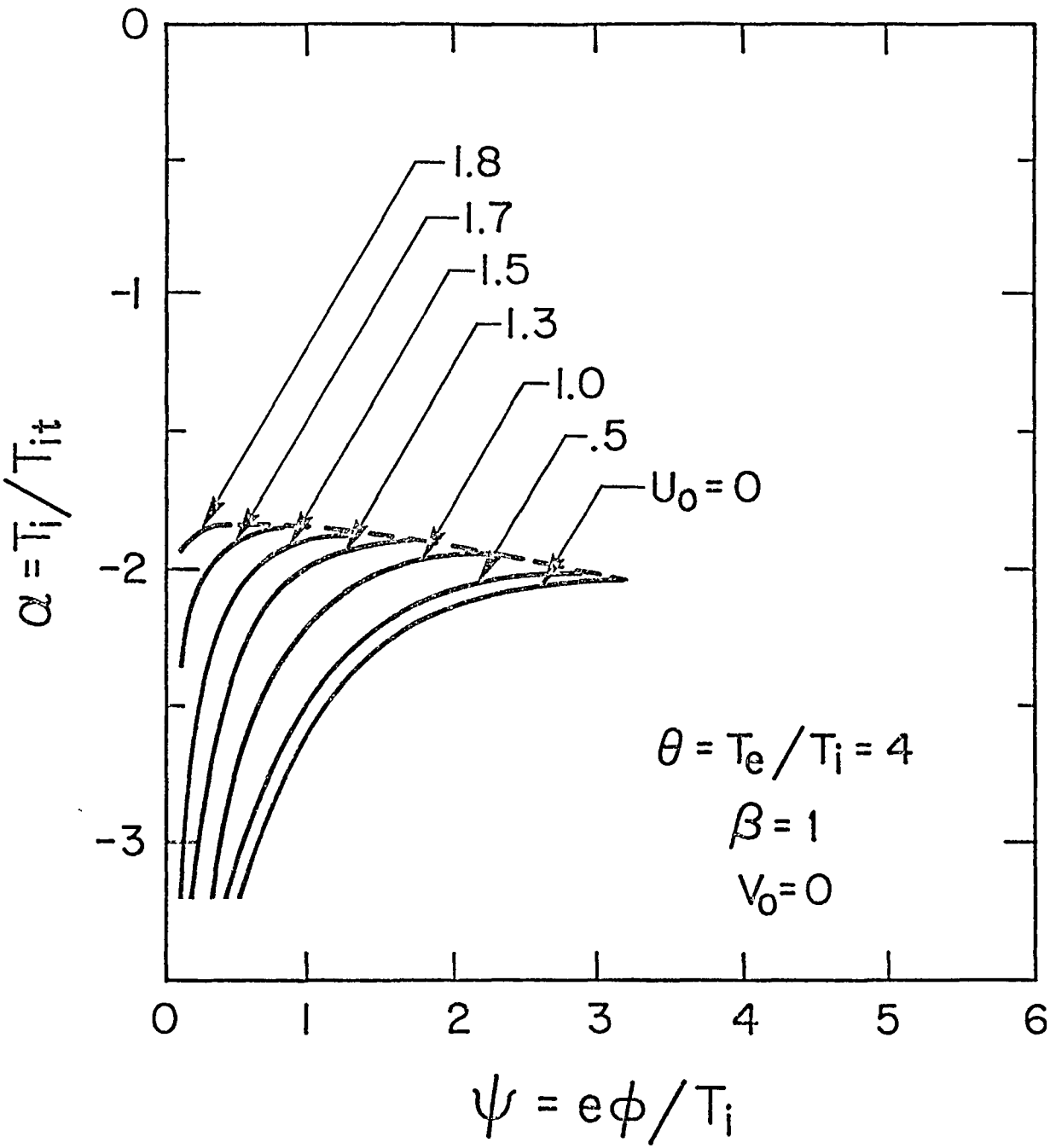
ION HOLES: 4 DISTRIBUTION FUNCTIONS
0
-1
-2
-3
1.8
1.7
1.5
1.3
1.0
.5
$U_0 = 0$
$\theta = T_e / T_i = 4$
$\beta = 1$
$V_0 = 0$
0
1
2
3
4
5
6
$\alpha = T_i / T_{it}$
$\psi = e\phi / T_i$

Fig. 5b

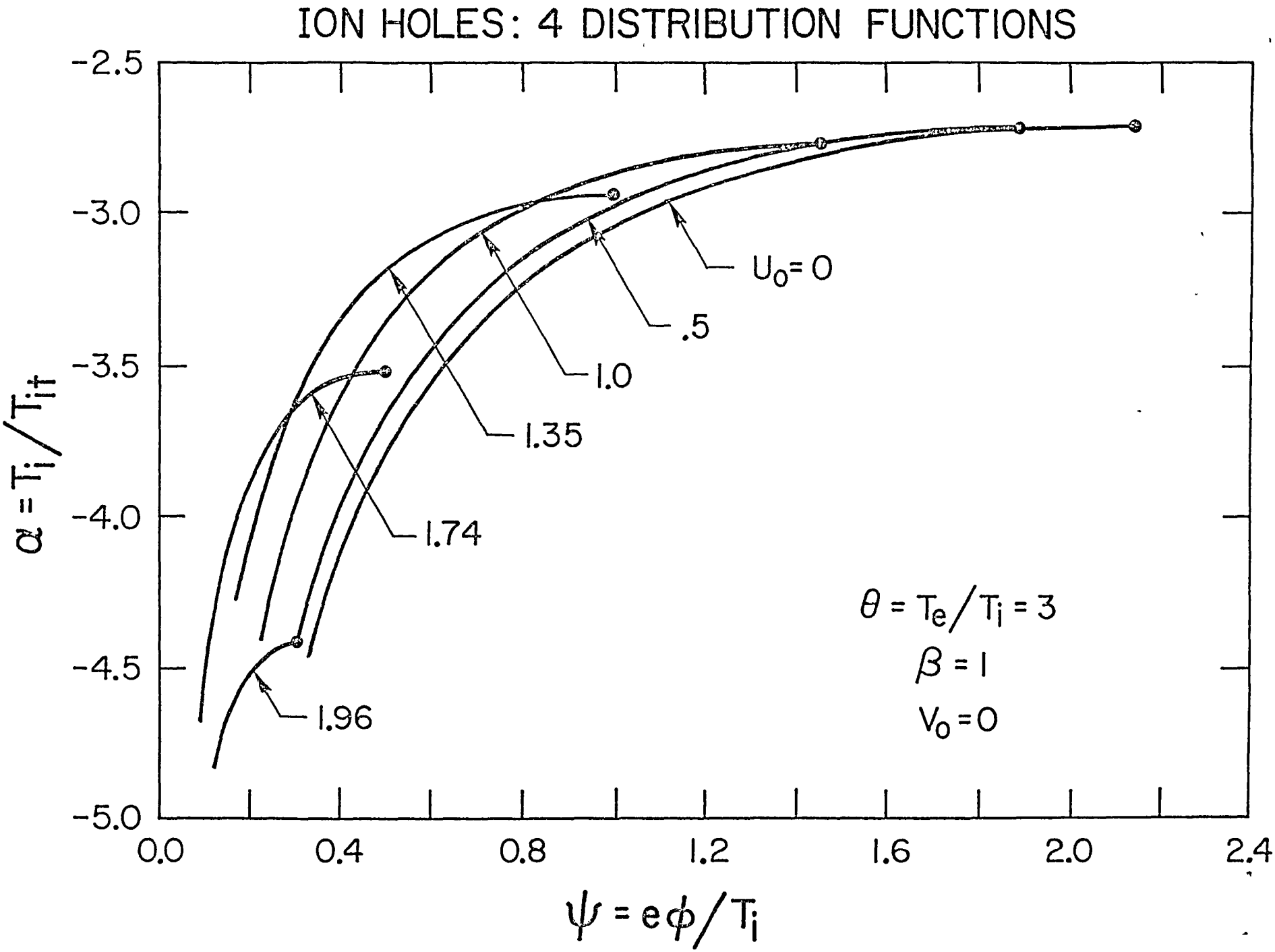
ION HOLES: 4 DISTRIBUTION FUNCTIONS
-2.5
-3.0
-3.5
-4.0
-4.5
-5.0
0.0
0.4
0.8
1.2
1.6
2.0
2.4
α = Ti/Tit
ψ = eφ/Ti
U0 = 0
.5
1.0
1.35
1.74
1.96
θ = Te/Ti = 3
β = 1
V0 = 0

Fig. 6

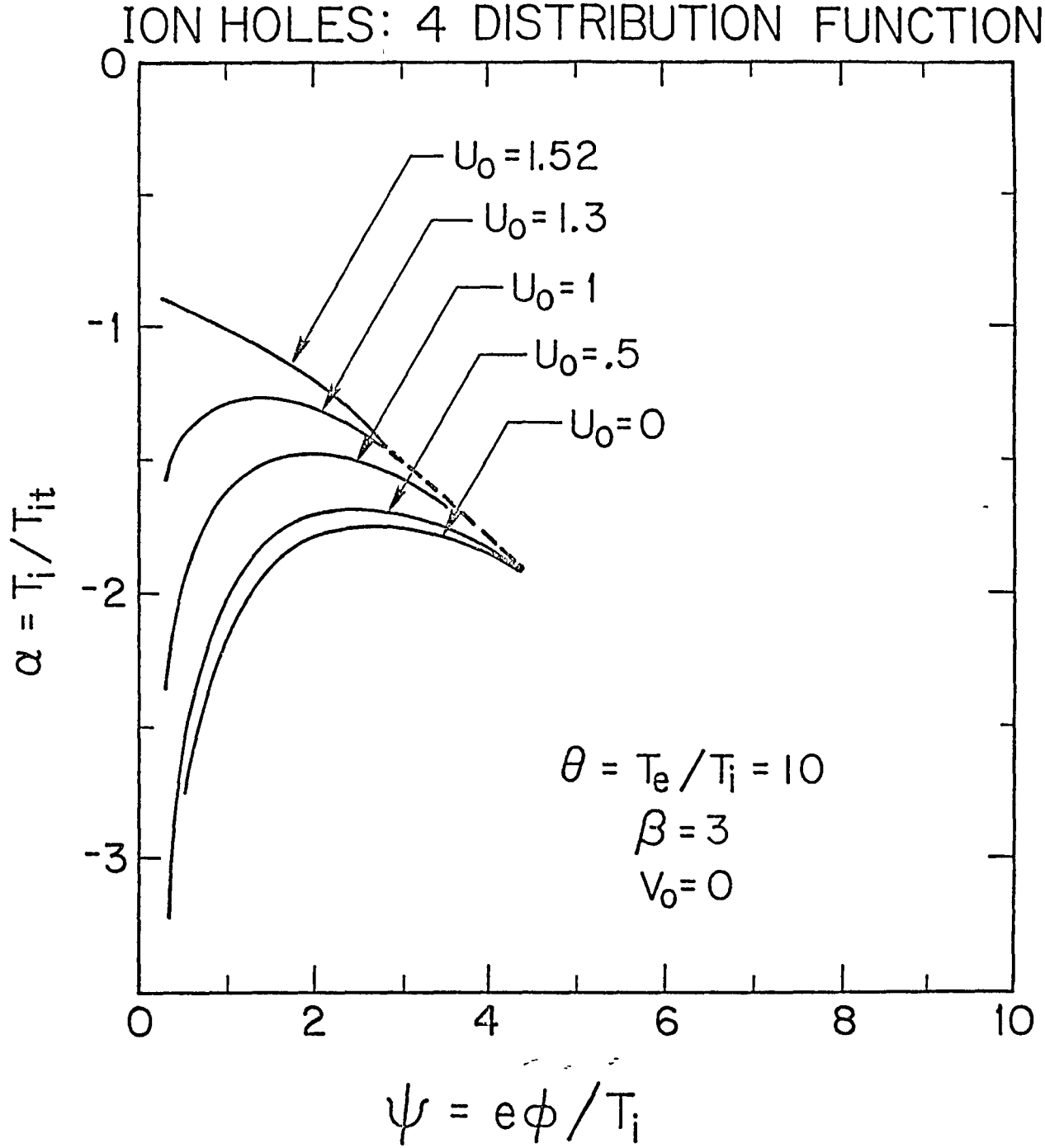
ION HOLES: 4 DISTRIBUTION FUNCTIONS
0
-1
-2
-3
$U_0 = 1.52$
$U_0 = 1.3$
$U_0 = 1$
$U_0 = .5$
$U_0 = 0$
$\alpha = T_i / T_{it}$
$\theta = T_e / T_i = 10$
$\beta = 3$
$V_0 = 0$
0
2
4
6
8
10
$\psi = e\phi / T_i$

Fig. 7

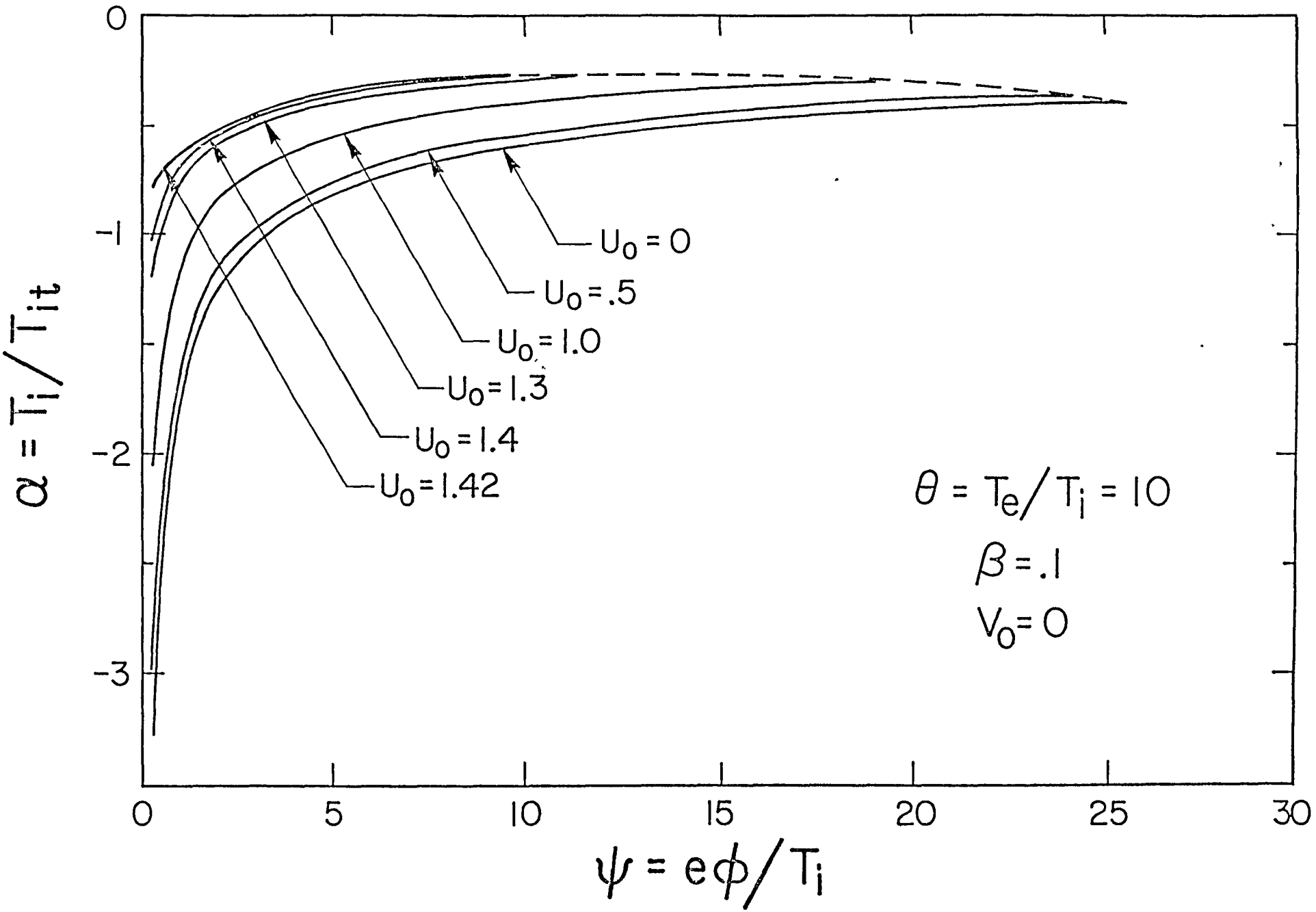
ION HOLES: 4 DISTRIBUTION FUNCTIONS
0
-1
-2
-3
$\alpha = T_i / T_{it}$
$U_0 = 0$
$U_0 = .5$
$U_0 = 1.0$
$U_0 = 1.3$
$U_0 = 1.4$
$U_0 = 1.42$
$\theta = T_e / T_i = 10$
$\beta = .1$
$V_0 = 0$
0
5
10
15
20
25
30
$\psi = e\phi / T_i$

Fig. 8

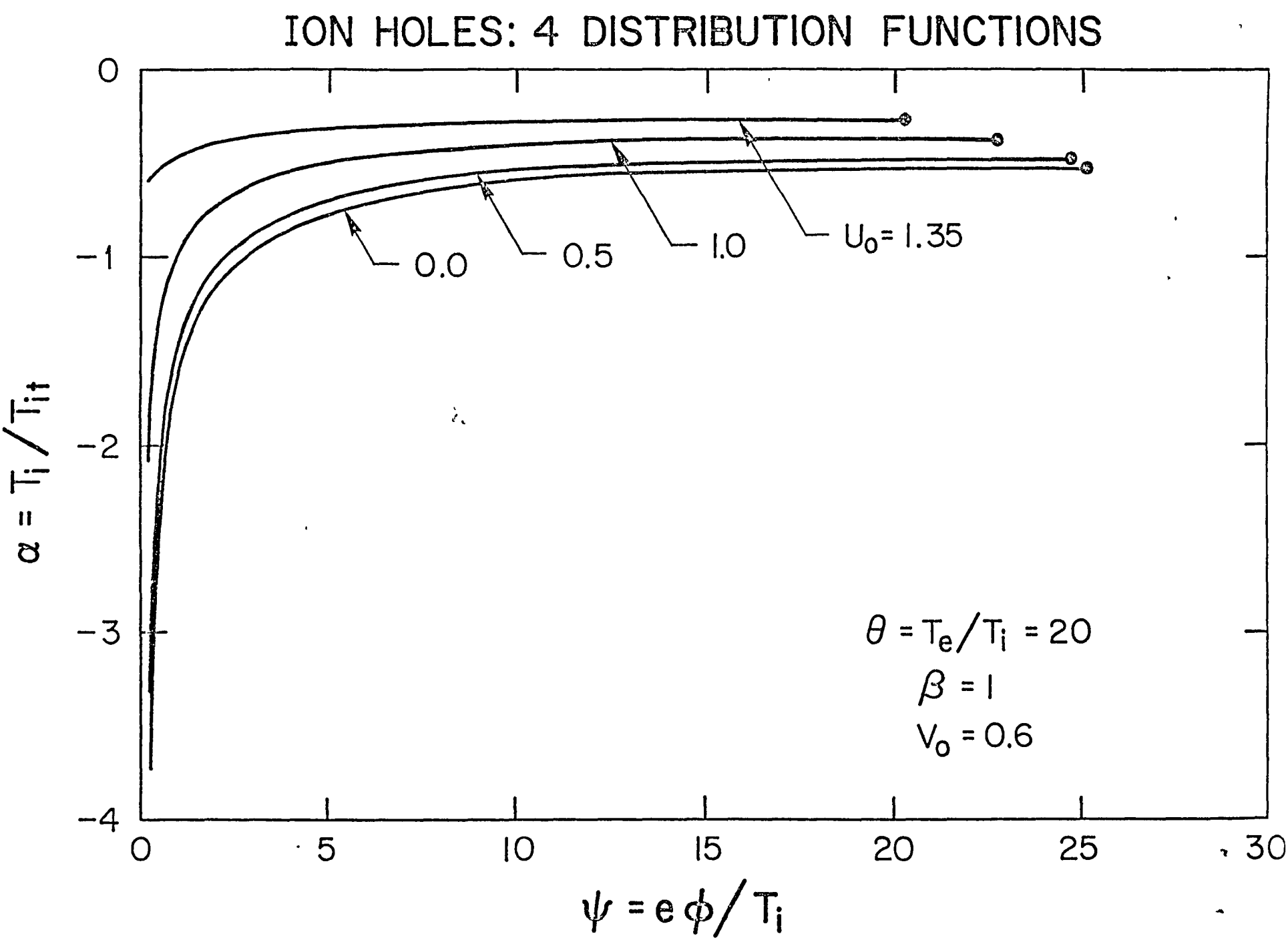
ION HOLES: 4 DISTRIBUTION FUNCTIONS
0
−1
−2
−3
−4
0
5
10
15
20
25
30
α = Ti / Tit
ψ = e φ / Ti
0.0
0.5
1.0
U0 = 1.35
θ = Te / Ti = 20
β = 1
V0 = 0.6

Fig. 9a

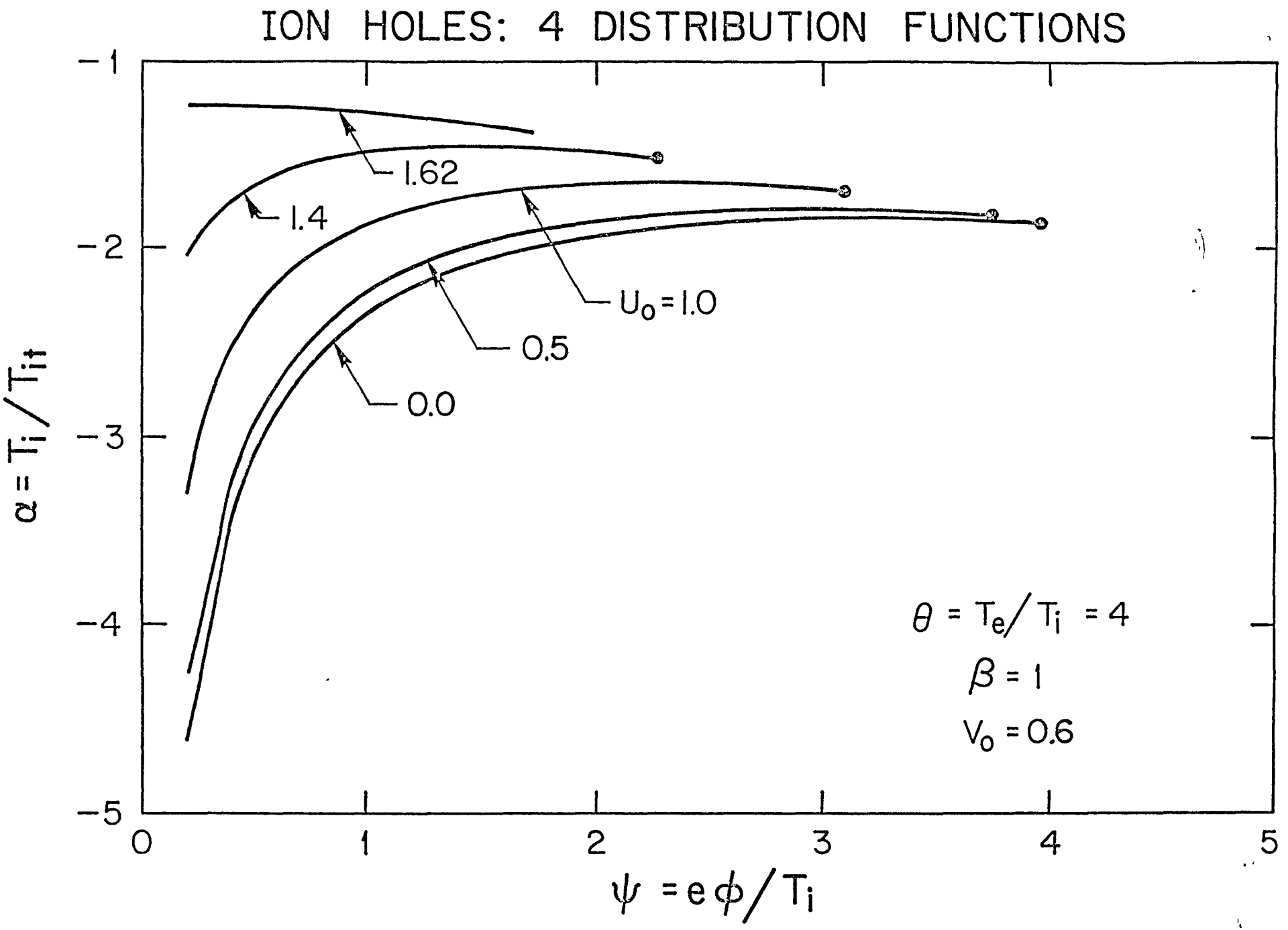
ION HOLES: 4 DISTRIBUTION FUNCTIONS
1.62
1.4
$U_0 = 1.0$
0.5
0.0
$\theta = T_e/T_i = 4$
$\beta = 1$
$V_0 = 0.6$
$\alpha = T_i/T_{it}$
$\psi = e\phi/T_i$
-1
-2
-3
-4
-5
0
1
2
3
4
5

Fig. 9b

End of Document